Injector Internal Geometry and Sub-Atmospheric Back Pressure Influence on Low Weber Number Liquid Flow

Nicolas Leboucher, Christophe Dumouchel, Denis Lisiecki, Yves Wanner

Injector Internal Geometry and Sub-Atmospheric Back Pressure Influence on Low Weber Number Liquid Flow

N. Leboucher, C. Dumouchel*, D. Lisiecki, Y. Wanner
CNRS UMR 6614 – CORIA, Université et INSA de Rouen, France
name@coria.fr

Abstract

The experimental work presented in this paper investigates the influence of the injector internal geometry on the primary atomization process in sub-atmospheric back pressure condition. A series of four injectors is studied. High-rate shadowgraph films of the liquid flow issuing from the nozzle are performed (66 667 fr/s). In order to have exploitable images, the injection pressure is maintained low (less than 1 MPa). On each image, the interface length per unit liquid surface area, $e_2(0)$, is measured. The examination of this parameter and of the images reveals that under atmospheric pressure, the primary atomization process is rather independent of the injectors. However, as the ambient pressure decreases, the injectors show different behaviour and the atomization process becomes intermittent. This behaviour is attributed to the apparition of cavitation in the injector. The characteristics of this intermittency are evaluated. Among other results, we observed that atomization process produced by cavitating flows are more sensitive to the injector internal geometry, the intermittency is due to the production of vortex cavitation, and, contrary to what is usually reported in the literature, cavitation does not enhance atomization in the present case. These results, as well as others, are presented and discussed in this paper.

Introduction

It is now well recognized that, whatever the injection pressure, the nature of the flow inside the injector influences primary atomization processes and the subsequent spray characteristics [1; 2]. It is therefore required to conduct specific investigations on the link between injector internal geometry and the liquid behaviour just at the nozzle exit. Such investigations must address also the important question concerning the characterization of atomizing liquid system.

The internal flow characteristics that are known to influence the issuing liquid flow are the distribution of velocity, the level of turbulence and the liquid cavitation. The velocity distribution, including axial and non-axial components, shapes the liquid flow. This is a very important step in atomization. Swirl injector is a well-known device based on this concept. It produces a thin conical sheet from the development of a high rotating motion inside the nozzle [3]. The turbulence of the issuing liquid flow imposes initial perturbations of different scales that structure the whole atomization process. In low-Weber atomization processes, the final spray characteristics are directly dependent on the initial turbulence level [4].

Liquid cavitation is a rupture in liquid continuum due to excessive stress and that appears as soon as the pressure decreases below the liquid vapour pressure. It is characterized by a change of phase of the liquid. Cavitation triggers in high injection pressure condition such as diesel or gasoline direct-injection and its effect on primary atomization processes has been widely investigated in these conditions [2]. Generally speaking, these investigations agree to say that cavitation enhances atomization but the reasons evoked to explain this are not fully established. Geometrically induced cavitation takes place at the nozzle orifice entrance and declines in three regimes, i.e., developing cavitation, super-cavitation, hydraulic flip [5]. Another type of cavitation structures due to the presence of hydrodynamic vortex in the liquid flow may also appear [6, 7]. The origin of these vortex or string cavitation structures has been experimentally investigated in injector up-scale model [8-10]. These investigations point out that string cavitation cannot exist in the absence of geometrically induced cavitation. It is more than probable that the influence of cavitation on the primary atomization depends on origin of cavitation.

According to the literature [12, 13] the appearance of geometrically induced cavitation imposes a stabilization of the mass flow rate as the back pressure decreases for a constant value of the injection pressure. This behaviour has been widely used to determine the condition of cavitation and the corresponding critical cavitation number. This number involves the injection pressure, the ambient pressure and the liquid vapour pressure. Numerous experimental results of the literature point out the dependence between the critical cavitation number and the injection pressure. Furthermore, the critical cavitation number shows that liquid cavitation can be triggered

* Corresponding author: Christophe.Dumouchel@coria.fr

by decreasing the ambient pressure [13]. In previous investigations addressing the influence of cavitation on liquid atomization processes, cavitation was always triggered by increasing the injection pressure.

In this experimental investigation, injections at low injection pressure are performed under sub-atmospheric pressure. Low injection pressure range is chosen in order to ease the visualization and analysis of the liquid flow at the nozzle exit, i.e., the initial step of the primary atomization process. Working at sub-atmospheric pressure allows getting rid of the aerodynamic effect and concentrating on the effect of the internal injector geometry. We expect that this will allow triggering liquid cavitation also. In this case, cavitation would be triggered at low injection pressure allowing its effect on the atomization process to be observable.

Experimental Setup and Diagnostics

The experimental setup is schematized in Fig. 1. The liquid is kept in a reservoir (fuel tank in Fig. 1) at the exit of which it is filtered. A combination of two pumps (low pressure LP and high pressure HP) provides an absolute injection pressure P_i ranging from 0 to 16 MPa and that is regulated and measured by a high pressure sensor just before the injector. The injector is fixed on top of a closed chamber in which the ambient pressure is controlled in the range [0.004 MPa; 0.2 MPa]. The interval chamber volume is 8.5 litres (23.4 x 19 x 19 cm^3). The chamber is equipped with four windows (one on each side, height: 12 cm; width: 8 cm). In order to limit liquid stagnation on the windows, an air-drift system sweeps each window by a controlled air-flow. The sub-atmospheric pressure in the chamber is controlled by a Sterling Pump (SIHI-Dry) that allows reaching 0.004 MPa. This pump can work even with contaminated air: the air does not have to be dry and the presence of liquid droplets is not penalizing.

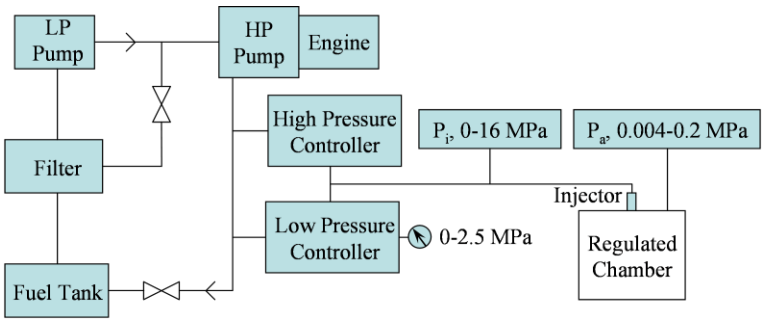

Figure 1 Experimental Setup

Injector Ref.	Characteristic
Inj. 1	Standard
Inj. 2	Smoothed inlet orifice
Inj. 3	Great needle roughness
Inj. 4	Great sac roughness

Table 1 Description and nomenclature of the injectors

A series of four injectors of the type of gasoline direct injection device is available. These injectors are conceived to work in transient conditions and are equipped with a needle controlling the closing and the opening of the injection device. In the closing position, the needle rests on the wall of the nozzle sac volume. The nozzle discharge orifices are located at the bottom of the sac volume. All injectors have three identical cylindrical orifices with the same diameter d_{or} = 190 µm and the same length, i.e., $L/d_{or} \approx 1$. These orifices are regularly distributed at the injector nozzle and make an angle of 23 degrees with the axis of the injector body. One of the injector is referred as standard (Inj. 1) and the three others present some differences concerning the orifice inlet profile (Inj. 2) and the roughness of the needle and of the sac (Inj. 3 and 4, respectively). The references of the injector are given in Table 1. When positioned on top of the chamber, the injector is orientated so that one of the jets injects vertically and can be fully observed through the window.

The liquid used is Shellsol D40 whose physical properties are close to those of gasoline. The liquid physical properties are: density ρ_L = 766 kg/m^3, surface tension σ = 0.025 N/m, dynamic viscosity μ_L = 0.9 10^{-3} kg/(ms), vapour pressure P_v = 300 Pa.

The present study focuses on the behaviour of the injector during the fully-open stage only and the transient opening and closing phases of the injector are ignored. During the fully-open stage, the needle has reached its upper position and the injector works in a steady state condition. The mass flow rate Q_m of the fully-open stage is measured for each injector as a function of the couple (P_i; P_a) by measuring the liquid mass $M(t_i)$ injected per injection as a function of the injection time t_i. (The injection time is defined as the duration of the electronic signal send to the injector.) For a fixed pressure drop $\Delta P_i = P_i - P_a$, this mass can be written as:

$$M(t_i) = Q_m t_{FO} + \Delta M(t_i) \quad (1)$$

where t_{FO} designates the time duration of the fully-open stage and $\Delta M(t_i)$ is the mass of liquid injected during the transient stages, i.e., during the opening and the closing of the injector. By assuming that $t_{FO} = t_i - \Delta t(t_i)$ where the time Δt might be a function of the injection time, Eq. (1) becomes:

$$M(t_i) = Q_m t_i + \Delta M(t_i) - Q_m \Delta t(t_i) \quad (2)$$

For great injection times, ΔM and Δt are independent of the injection time and therefore, according to Eq. (2), $M(t_i)$ increases linearly with t_i and the mass flow rate is the slope of this evolution. Thus, Q_m is obtained by measuring $M(t_i)$ for a range of sufficiently large injection times, i.e., greater than 2 ms. The discharge coefficient C_D of the injector fully-open stage is then calculated by $C_D = 4Q_m / (3\pi d_{or}^{\ 2} \sqrt{2\rho_L \Delta P_i})$.

High-speed shadowgraph images of the jet issuing from the injectors are performed with a Phantom V12.1 Camera (256x256 pixels). The acquisition rate is fixed at 66 667 frames/s corresponding to a time delay of 15 µs between consecutive images and the exposure time is 0.3 µs. The physical field covered by the optical arrangement is 2.6 mm x 2.6 mm which makes a spatial resolution equal to 10 µm/pixel. The light source is a continuous 300 W Xenon arc source.

In complement to the high-speed films, shadowgraph snapshots are performed with a camera MatrixVision (1600 x 1200 pixels) which offers a high spatial resolution and a nanolite light source. In this second configuration, the light source has a time duration equal to 20 ns and plays the role of the shutter. The physical field covered with this second optical configuration is 6 mm x 8 mm corresponding to a spatial resolution equal to 5 µm/pixel.

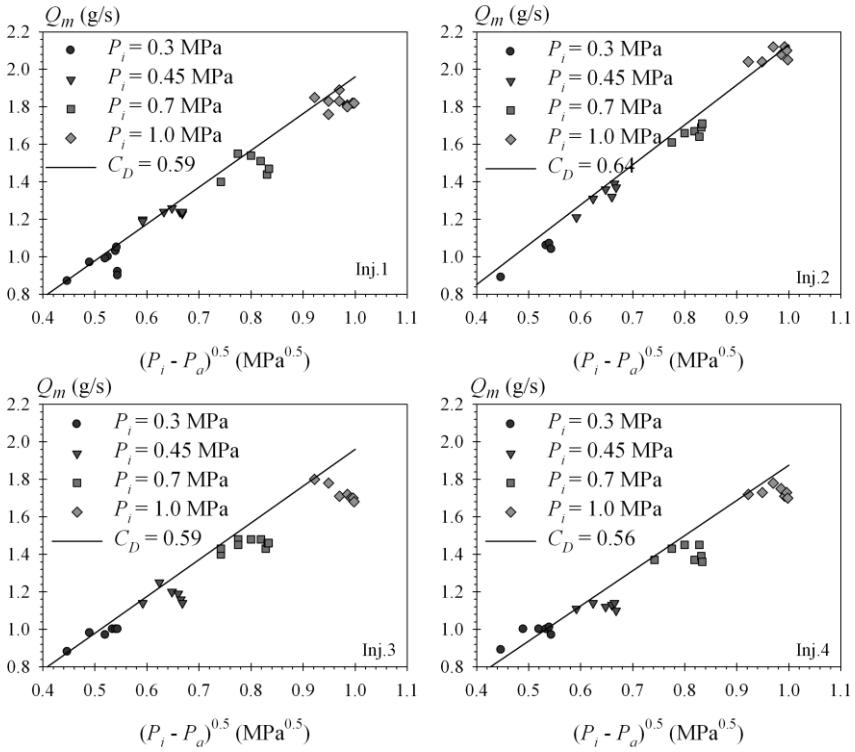

Figure 2 Fully-open stage mass flow rate as a function of the injection and ambient pressures P_i and P_a (the line illustrates the dependence with the discharge coefficient measured under atmospheric pressure P_a = 0.1 MPa)

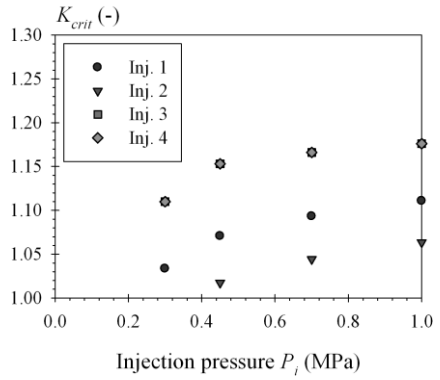

Figure 3 Estimation of K_{crit} for each injector

Experimental Results

Figure 2 presents the mass flow of the fully-open stage as a function of the injection and ambient pressures. The point series shown in the graphs of this figure correspond to specific injection pressure P_i and the increase of pressure drop is obtained by reducing the ambient pressure. For each injector, the discharge coefficient measured under atmospheric pressure is indicated in each figure as well as the relationship it imposes between the pressure drop and the mass flow rate. Inj. 2 shows the greatest discharge coefficient. Experimental investigations of the literature reported greater discharge coefficients for cylindrical discharge orifices with rounded inlet geometry [14]. The present observation agrees with this behaviour. We note however that the increase of the discharge coefficient for Inj. 2 is moderate compared to what is reported in the literature which is likely due to the fact that its orifice-inlets have been smoothed but not fully rounded.

For each injector, Fig. 2 highlights a saturation of the mass flow rate as the relative injection pressure increases. According to the literature [1, 11, 12] the stabilization of the mass flow rate as the ambient pressure decreases has been reported is due to the apparition of cavitation in the injector. In these works, the injec-

tion pressure is usually great (above 10 MPa) and the ambient pressure is reduced from this value to the atmospheric pressure. We see here that working at low injection pressures with ambient pressures below the atmospheric reports similar behaviour. Except for Inj. 2, note that for P_i = 1.0 MPa, the stabilization of the mass flow rate occurs at atmospheric pressure. Therefore, the presence of cavitation at this injection pressure seems probable. Following Payri's methodology [1, 11, 12], we estimate the critical cavitation number K_{crit} under which cavitation occurs as the number $K = (P_i - P_v)/(P_i - P_a)$ where P_a is given the value at which mass flow rate stabilization occurs. The results are presented in Fig. 3. As reported elsewhere [1, 11, 12], we find that K_{crit} increases with the injection pressure. Figure 3 shows that K_{crit} depends on the injector internal geometry also: cavitation takes place less easily in the smoothed orifice inlet injector and more easily in the devices with greater roughness.

Figure 2 indicates also that, when the mass flow rate stabilization is reached, further decrease of the ambient pressure induces a decrease of the mass flow rate. This behaviour, which has not been observed by others, clearly evidences a strong modification of the internal liquid flow that should have repercussion on the atomization process. Examination of images of the liquid flow at the nozzle exit confirms this point.

Examples of images extracted from high-speed films are presented in Fig. 4. These images show the influence of P_a on the atomization process when P_i = 0.3 MPa for Inj. 1 and Inj. 4. These images show two different atomization processes. AP1: The jet issuing from the injector shows a highly perturbed interface with the emergence of lateral ligaments that ensure an early disintegration. AP2: The liquid system issuing from the injector is much wider than in AP1 and the lateral ligaments are far less developed and totally absent sometimes. Breakup and drop formation seem to be delayed compared to AP1. The presence of each atomization process is dependent on the ambient pressure and on the injector. At P_a = 0.1 MPa, only AP1 is observed whatever the injection pressure and the injector. For ambient pressure of 0.01 MPa and less, the liquid atomization process is intermittent between AP1 and AP2. The percentage rate of each atomization process will be estimated later but note in Fig. 4, that for the lowest ambient pressure, Inj. 4 reported the AP2 only.

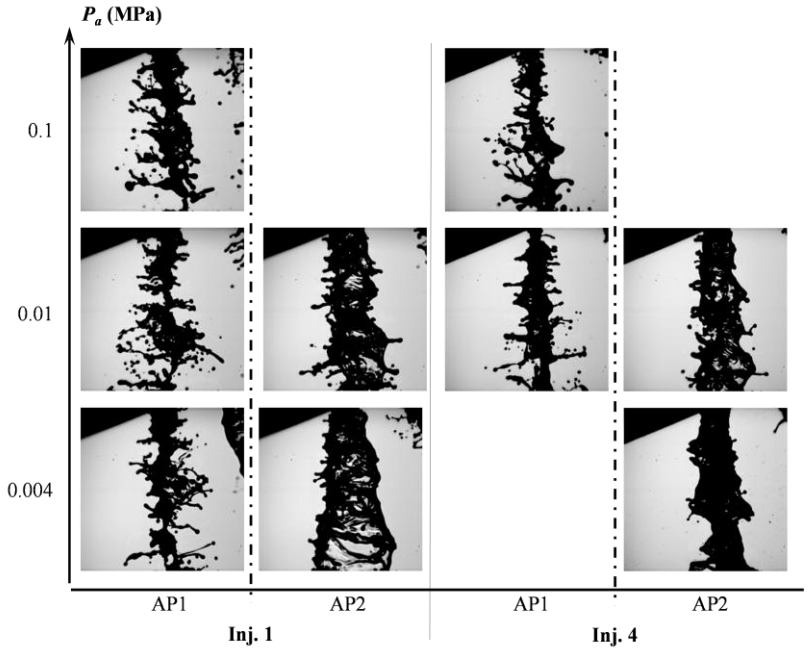

Figure 4 Images from the high-speed films. Influence of the ambient pressure on the liquid flow issuing from the injector (P_i = 0.3 MPa, AP1: Atomization process 1; AP2: Atomization process 2)

The emergence of AP2 in Fig. 4 is not due to an increase of the pressure drop when the ambient pressure decreases. To illustrate this Fig. 5 presents two images for a constant pressure drop (ΔP_i = 0.3 MPa) at two different ambient pressures (0.1 and 0.004 MPa). These images are snapshots and concern Inj. 1. At P_a = 0.1 MPa only AP1 has been observed (left image in Fig. 5). At P_a = 0.004 MPa, the second atomization process has been observed intermittently (right image). Therefore, the triggering of AP2 is well related to the decrease of the ambient pressure.

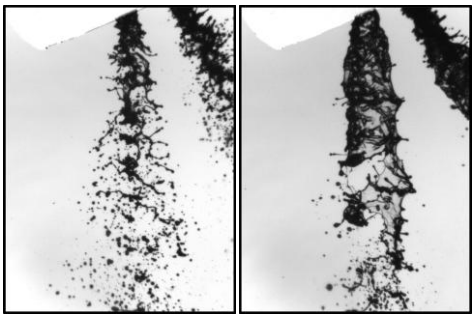

Figure 5 Snapshots of liquid system produced by Inj. 1 (ΔP_i = 0.3 MPa, left: P_a = 0.1 MPa, right: P_a = 0.004 MPa)

The intermittency between AP1 and AP2 during the injection motivated performing high-speed films in order to estimate the appearance rate of each process. To achieve this, the film images were treated and transformed into two grey levels images on which liquid appears in black on a white background. Using classical image treatment tools, the boundary of the continuous liquid system, i.e., the one attached to the nozzle, is detected. The length L of this bound-

ary is measured as well as the surface area A_s it delimits. Each image is characterized by the ratio:

$$e_2(0) = \frac{L}{2A_s} \tag{3}$$

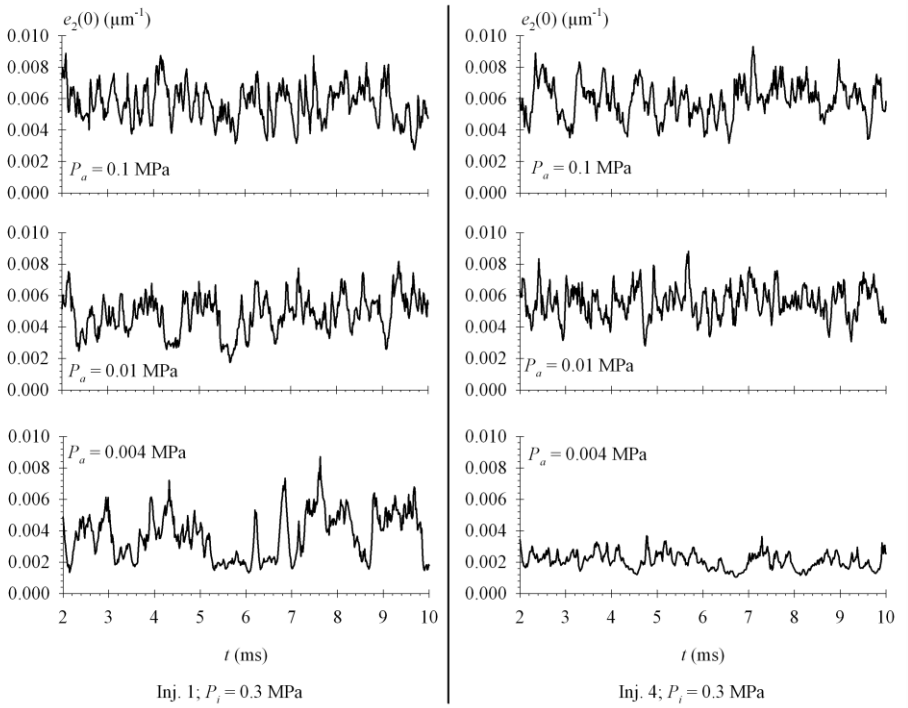

Figure 6 Temporal evolution of $e_2(0)$ as a function of the ambient pressure (P_i = 0.3 MPa, left: Inj. 1, right: Inj. 4)

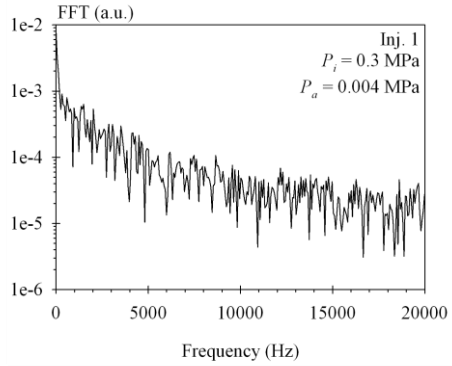

Figure 7 FFT of the $e_2(0)$ temporal signal (Inj. 1, P_i = 0.3 MPa, P_a = 0.004 MPa)

This ratio is noted $e_2(0)$ since it corresponds to the value of the surface-based scale distribution $e_2(D)$ for the scale $D = 0$ [15]. This distribution has been used to characterize atomization processes and to develop new atomization models [15, 16]. $e_2(0)$ corresponds to the amount of interface per unit area of surface which is an interesting information in liquid atomization: efficient atomization processes show great value of $e_2(0)$. If we go back to the identification of AP1 and AP2 (Fig. 4) we see that the very deformed jets of AP1 should be characterized by greater values of $e_2(0)$ than those of AP2 that are much wider (A_s is greater) and less tortuous (L is smaller). For the operating conditions shown in Fig. 4, Fig. 6 presents the temporal evolution of the ratio $e_2(0)$. The signals obtained at P_a = 0.1 MPa characterize the atomization process AP1: $e_2(0)$ oscillates between 0.004 and 0.008 and does not report significant differences between Inj. 1 and Inj. 4. (The mean of $e_2(0)$ are equal to 0.0056 and 0.0059 for Inj. 1 and 4 respectively.) At P_a = 0.01 MPa, some differences arise: the Inj. 4 signal is not very different than the one obtained for the greater ambient pressure but the Inj. 1 signal shows two major differences. First, the $e_2(0)$ values are not as great as for P_a = 0.1 MPa and, second, we note that at around 2.5, 4.5 and 5.5 ms, $e_2(0)$ collapses during a small time interval. This behaviour is the mark of the triggering of AP2. It is not reported for Inj. 4. (We must add here that as far as the appearance of each atomization process is concerned, differences from one injection to another could be observed.) Finally, for the lowest ambient pressure P_a = 0.004 MPa, the difference between Inj. 1 and Inj. 4 is much more pronounced. For Inj. 1, we see that AP2 lasts longer, whereas for Inj. 4, AP2 is stable during the all injection. We can add here, that, as illustrated in Fig. 7, no specific frequency was reported whatever the operating conditions including the injection, the injection pressure and the ambient pressure: the intermittency between AP1 and AP2 is not related to a specific frequency. Note that the absence of frequency is a characteristic of super-cavitation regime [13].

Generally speaking, a similar behaviour was observed for the other injectors. Figure 8 compares the number fraction distribution of $e_2(0)$ for each injector at the two extreme ambient pressures and a constant injection pressure (P_i = 0.3 MPa). These distributions are produced from the temporal evolution of $e_2(0)$ as those shown in

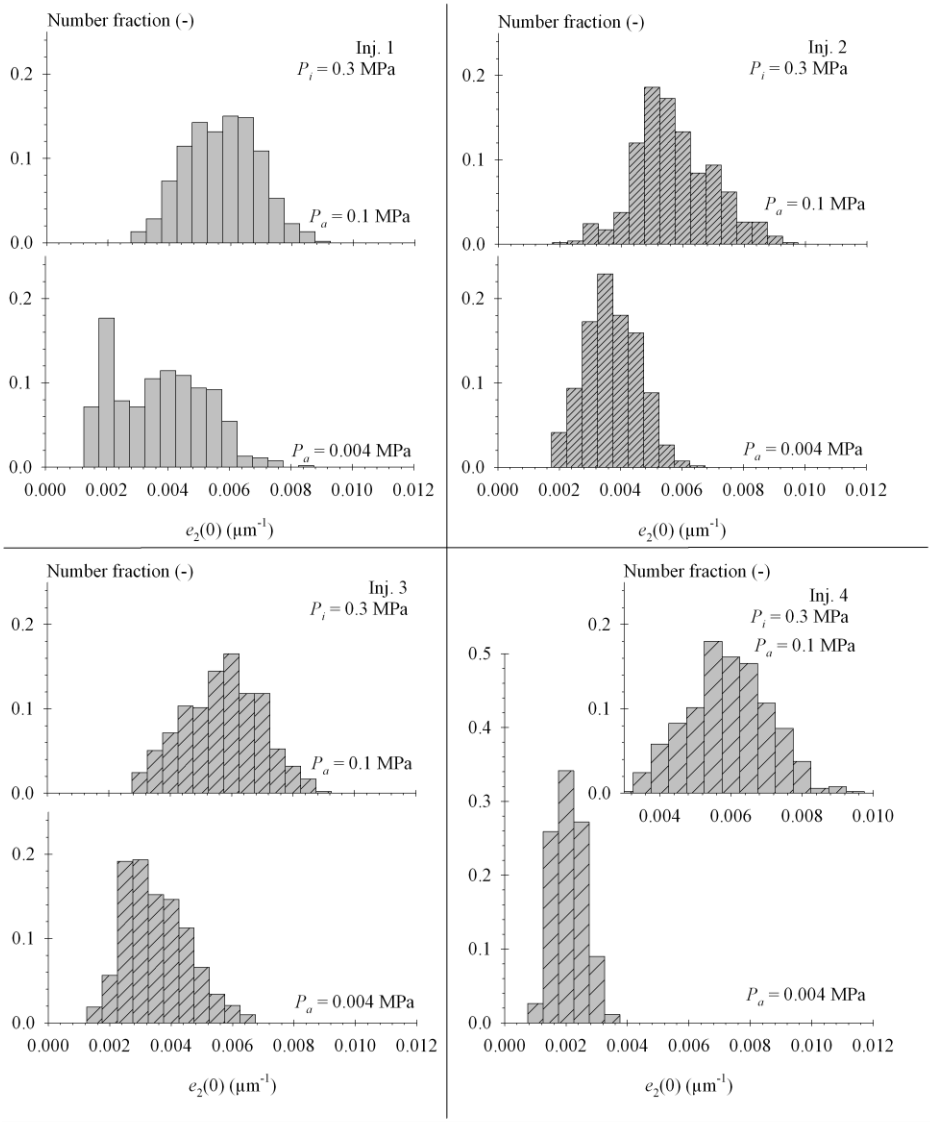

Figure 8 Number fraction distribution of $e_2(0)$. Influence of the injector and of the ambient pressure (P_i = 0.3 MPa)

Fig. 6 for one injection only. Note first that the four injectors present very similar $e_2(0)$ distributions under atmospheric pressure. Indeed, the four distributions for this ambient pressure are mono-modal, almost symmetrical and spread on a similar interval of $e_2(0)$. For the smallest ambient pressure, differences between the four injectors are numerous. The distribution reported by Inj. 1 clearly shows two peaks corresponding to the two atomization processes. Note that the right peak (corresponding to AP1) has been left shifted with the decrease of the ambient pressure. The distributions reported by Inj. 2 and Inj. 3 are still mono-modal but they are narrower and left shifted compared to those obtained at atmospheric pressure. For these two injectors, the atomization process intermittency between AP1 and AP2 has been observed but the values of $e_2(0)$ of each process seem to be too close to each other (as discussed later) to generate a bi-modal distribution in Fig. 8. Finally, the distribution obtained for Inj. 4 is very narrow and located at a small value of $e_2(0)$. This result is representative of the atomization process AP2 which is stable for this operating condition (see Fig.6).

P_a (MPa)	Inj. 1		Inj. 2		Inj. 3		Inj. 4	
	AP1	**AP2**	**AP1**	**AP2**	**AP1**	**AP2**	**AP1**	**AP2**
0.004	*50%*	*50%*	55%	45%	40%	60%	*0%*	*100%*
	0.0048	*0.0026*	0.0042	0.0033	0.0043	0.0030	-	*0.0023*
0.01	80%	20%	90%	10%	95%	5%	*95%*	*5%*
	0.0051	0.0034	0.0050	0.0035	0.0056	0.0035	*0.0056*	*0.0032*-
0.1	*100%*	*0%*	100%	0%	100%	0%	*100%*	*0%*
	0.0056	-	0.0058	-	0.0058	-	*0.0059*	-

Table 2 Estimation of the percentage of each Atomization Process and corresponding average value of $e_2(0)$ (µm^{-1}) (P_i = 0.3 MPa, Figures in italic indicate average performed on five injections)

In complement to the results presented in Fig. 8, the estimations of percentage of each atomization process as well as the corresponding average values of the ratio $e_2(0)$ have been determined. The results are gathered in Table 2. It is important to add here that the percentage of presence of each atomization process might report significant variations from one injection to another. This is the reason why the accuracy of the percentage shown in Table 2 is low (5%) and that the results for three ambient pressures (the lowest, the greatest and a medium value) are reported only. We believe however that this percentage gives interesting indications. On the other hand, we noticed that the average values of $e_2(0)$ obtained for each atomization process is rather well reproducible from one injection to another.

As already mentioned, Table 2 reminds that, whatever the injector, the atomization process AP1 is the only one observed when P_a = 0.1 MPa. It is also interesting to note that for this case, the average value of $e_2(0)$ during the fully-open stage is not very much dependent on the injector. As the ambient pressure decreases, several observations can be made. First, the AP1-percentage decreases and the AP2-percentage increases. Note that these variations (which are estimations as pointed out above) depend on the injector as well as on the ambient pressure. At P_a = 0.004 MPa, the smallest AP2-percentage is obtained for Inj. 2. This injector has the lower critical cavitation number (see Fig. 3) indicating a lower propensity to trigger cavitation. Similarly, the injectors with the greatest critical cavitation number (Inj. 3 and 4) report the greatest percentage of AP2 at P_a = 0.004 MPa. As observed in Fig. 8, the mean value of $e_2(0)$ for AP1 and AP2 are close to each other for Inj. 2 and 3. This is the reason why, the distribution for these injectors in Fig. 8 are mono-modal. The evolution of the average of $e_2(0)$ with P_a is also instructive. We see that, for the two atomization processes, the average of $e_2(0)$ decreases with the ambient pressure. This means that, whereas the pressure drop increases (since P_i is constant), the primary atomization process seems to be less and less effective when P_a decreases, i.e., when cavitation is triggered. This observation is unusual since it is generally admitted that cavitation globally enhances atomisation. This behaviour is not observed in the present working conditions. Finally, it is interesting to note that the characteristics of the atomization processes at the lowest ambient pressure including the percentage of each process and the corresponding average of $e_2(0)$ depend on the injector. As said above, this is not the case under atmospheric pressure. This indicates that, as cavitation is triggered, the atomization process becomes sensible to injector characteristics that have a negligible influence otherwise. Of course this last result should be confirmed by proper spray drop-size distribution measurements. This point is currently under consideration.

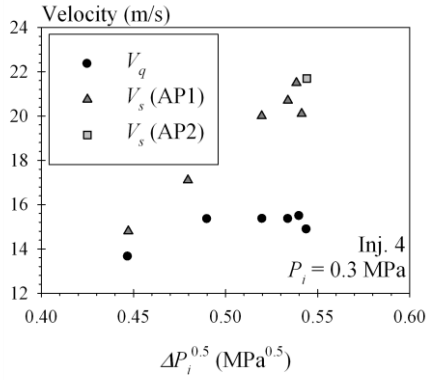

Figure 9 Comparison between average velocity V_q and the structure velocity V_s (Inj. 4, P_i = 0.3 MPa)

Finally, high-speed films allow estimating the velocity V_s of liquid ligaments and structures just downstream the exit section. These estimations have been performed for Inj. 4 at different ambient pressures by taking five couples of images and by measuring on each couple 10 velocities V_s by recognizing liquid structures on each image. The structure velocities are shown in Fig. 9 where mass-flow rate velocities V_q (evaluated from the mass flow rate and the section of the orifices) are also represented. Whereas these two velocities are of the same order of magnitude under atmospheric condition, we see that V_s is always far greater than V_q when the ambient pressure decreases. Since no acceleration of the liquid from the nozzle exit to the position where images were taken is possible, this difference indicates that the issuing flow occupies a portion of the nozzle exit section only. This behaviour is a known characteristic of cavitating flows. We note also that the structure velocity shows a linear relationship with the square root of the pressure drop. For cavitating flow, such behaviour is observed for the effective velocity [1]. The correspondence between the effective and the liquid structure velocity would suggest flow detachment from the orifice wall down to the nozzle exit section and therefore an independency between the atomization process and the structure velocity. As far as this point is concerned, it is important to remind here the very short length of the nozzle discharge orifice and to point out that, as illustrated in Fig. 9, V_s doesn't vary much with the atomization process.

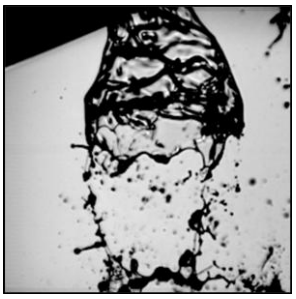

Figure 10 Image at the end of the injection (Inj. 4, P_i = 1.0 MPa, P_a = 0.004 MPa)

Finally, considering the value of the structure velocity for the atomization process AP2 as well as the width of the liquid flow in this condition (see Fig. 4 for instance), it can be shown that the structure of the flow for this atomization process is likely an annular liquid sheet. Visualization of the liquid jet at the end of the injection (Fig. 10) confirms the axisymmetric and hollow structure of the liquid flow.

Summary and Conclusions

The present experimental investigation shows that even in the absence of aerodynamic forces, i.e., at low injection pressure, the ambient pressure may have an important influence on the liquid atomization process. This influence is due to a deep modification of the injector internal liquid flow. Several points indicate that this modification is due to the apparition of liquid cavitation: as the ambient pressure decreases, the mass flow rate stabilizes, the atomization process becomes intermittent and the velocity of the issuing liquid flow is much greater than the average mass flow-rate velocity. Indeed, according to Payri's works, mass flow rate stabilization as the pressure drop increases is a characteristic of cavitation. Several observations underlined the highly unstable nature of cavitating flows [5, 13, 17]. Finally, cavitating flows may not cover the whole orifice section which results in velocity greater than the flow-rate mean velocity [1]. Thus, this demonstrates that the influence of cavitation on liquid atomization process can be investigated at low injection pressure, i.e., in a condition for which the qualification and quantification can be approached by visualizations and image analyses as done here. In the present investigation, the atomization processes are identified by their interface length per unit of liquid surface area. This information is important in atomization and succeeds in identifying and quantifying different processes. It is observed that cavitation triggers an intermittent liquid atomization process and that the characteristics of this intermittency are functions of the injector internal geometry. This intermittency is never related to a given frequency. A similar result was reported in super cavitation regime [13]. This regime is characterized by a propagation of the cavitation structures down to the nozzle exit section. One of the important geometrical characteristics of the injector investigated here is the small discharge orifice length that is likely in favour of the apparition of a super cavitation regime.

In this work, the intermittency is characterized by an alternation between two atomization processes. One of them corresponds to the production and atomization of an annular liquid sheet. This specific geometry is believed to result from the development of string or vortex cavitation [8-10]. These structures, which are known to be very unstable, find their origin in the vortex development in the nozzle sac volume of multi-hole injectors. Our injectors are equipped with such a region.

As far as the efficiency of the atomization processes is concerned we find that it becomes more sensitive to injector internal geometrical characteristics in case of cavitation and that, contrary to what is often reported, it seems to be not enhanced by cavitation. Although it has to be corroborated by proper spray characterisation, this last observation is believed to be related to the absence of reattachment of the liquid flow in the discharge orifices because of their too short length. Thus, turbulence is considerably reduced and the subsequent initial perturbation level of the liquid flow at the nozzle exit is low.

Acknowledgements

The authors thank MAGIE FUI project for the financial support.

References

[1] Desantes, J.M., Payri, R., Pastor, J.M., Gimeno, J., Atom. Sprays 15: 489-516 (2005)
[2] Dumouchel, C., Exp. Fluids 45: 371-422 (2008)
[3] Lefebvre, A.H., *Atomization and Sprays*, Hemisphere Publishing Corporation, New-York (1989)
[4] Dumouchel, C., Cousin, J., Triballier, K., Exp. Fluids 38 : 637-647 (2005)
[5] Sou, A., Hosokawaa, S., Tomiyama, A., Int. J. Heat Mass Trans. 50: 3575-3582 (2007)
[6] Soteriou, C., Andrews, R., Torres, N., Smith, M., Kunkulagunta, R., ILASS-Europe 2001, Zürich, 2-6 September 2001
[7] Arcoumanis, C., Gavaises, M., Flora, H., Roth, H., Mec. Ind. 2: 375-381 (2001)
[8] Andriotis, A., Gavaises, M., Arcoumanis, C., JFM 610: 195-215 (2008)
[9] Andriotis, A., Gavaises, M., Atom. Sprays 19: 247-261 (2009)
[10] Gavaises, M., Andriotis, A., Papoulias, D., Mirologlou, N., Theodorakakos, A., Phys. Fluids 21: 052107 (2009)
[11] Payri, R., Guardiola, C., Salvador, F.J., Gimeno, J., Experimental Techniques 28: 49-52 (2004)
[12] Payri, F., Bermudez, V., Payri, R., Salvador, F.J., Fuel, 83: 419-431 (2004)
[13] Stanley, C., Barber, T., Milton, B., Rosengarten, G., Exp. Fluids 51: 1189-1200 (2011)
[14] Ohrn, T.R., Senser, D.W., Lefebvre, A.H., Atomization and Sprays, 1: 137-153 (1991)
[15] Dumouchel, C., Grout, S., Int. J. Multiphase Flow, 35: 952-962 (2009)
[16] Dumouchel, C., Grout, S. Physica A 390: 1811-1825 (2011)
[17] Sato, K., Saito, Y., JSME Int. J. 45: 638-645 (2002)